The Role of Surface Termination Geometry on the Ground-State and Optical Properties of Silicon Nano-Crystals: A Density Functional Theory Study

Sanaz Nazemi*, Ebrahim Asl Soleimani*, Mahdi Pourfath*† Hans Kosina†
*School of Electrical and Computer Engineering, University of Tehran, Tehran 14395-515, Iran
†Institute for Microelectronics, Technische Universität Wien, Wien A-1040, Austria
Email: pourfath@ut.ac.ir & pourfath@iue.tuwien.ac.at

***Abstract*—Silicon nano-crystals (NC) are potential candidates for enhancing and tuning optical properties of silicon for opto-electronic and photo-voltaic applications. Due to the high surface-to-volume ratio, however, optical properties of NC result from the interplay of quantum confinement and surface effects. In this work, we show that both the spatial position of surface terminants and their relative positions have strong effects on NC properties as well. This is accomplished by investigating the ground-state HOMO-LUMO band-gap, the photo-absorption spectra, and the localization and overlap of HOMO and LUMO orbital densities for prototype $Si_{32}H_{42}$ NC. It is demonstrated that the surface passivation geometry significantly alters the localization center and thus the overlap of frontier molecular orbitals, which correspondingly modify the electronic and optical properties of NC.**

***Keywords*—Silicon nano-crystals, surface passivation, time dependent density functional perturbation theory**

I. Introduction

The combination of non-toxicity, abundance, low cost and rather simple processing have made Si as the base-material for semiconductor technology [1]. Crystalline Si is not suitable for optical applications, because of its indirect band-gap. If the size of the system approaches the wavelength of carriers, however, tails of electron and hole wavefunctions partially overlap that gives rise to quasi-direct transitions and thus improving optical properties of silicon [2]. In NCs which are smaller than the exciton Bohr radius of the material (∼5 nm for Si) the optical gap is inversely proportional to the dimension of the structure [3], [4]. However, due to high surface-to-volume ratio in NCs, surface effects become important. Intensive experimental and theoretical studies on parameters that affect optical properties of Si NCs have been performed over the past two decades [5]–[9]. Chemical nature of the surface including the passivant material and its bonding type have shown to be strongly effective on the optical properties of NC. Using quantum Monte Carlo calculations, Puzder et al. [7] have shown that double bonded surface passivant groups, specifically oxygen atoms, significantly reduce the optical gap of Si NCs, while single bonded groups have a minimal influence. Nurbawono et al. [5] have utilized time dependent density functional tight binding (TDDFTB) model to demonstrate that the absorption spectra of Si NCs can be tuned with small molecule passivations such as methyl, hydroxyl, amino, and fluorine. To the best of our knowledge, a comprehensive study of the effect of the relative position of surface passivants on NC properties is missing. In this work time (in)dependent density functional theory simulations have been utilized to analyze the role of spatial position of surface passivants on the optical gap of NC. The paper is organized as follows: Sec. II describes the employed computational method, Sec. III discusses the effect of spatial configuration of surface passivation on the HOMO/LUMO density distributions and the optical absorption spectra of $Si_{32}H_{42}$ NC. Finally, concluding remarks are presented in Sec. IV.

II. Structures and Methods

a) Model Structure: In medium and large sized NCs, the crystallographic planes form facets [10] (see Fig. 1 (a)). Thus, in this work Si NCs are defined as Wulff-constructions with (100), (110) and (111) facets, cut out from the FCC crystal lattice of bulk Si. The studied NCs have diameters in the range of ∼1.2-2.4 nm with surface dangling bonds that are hydrogen passivated.

b) Calculation Approach: Lattice structures have been relaxed using conjugate gradient calculations within density functional theory (DFT) as implemented in SIESTA code [11]. Norm conserving pseudo-potentials along with the numerical atomic orbitals with double zeta polarized basis set and a mesh cutoff of 55 Ry have been used. The Kohn-Sham equations have been solved in the framework of generalized gradient approximation (GGA) with Perdew-Burke-Ernzerhof (PBE) exchange-correlation functionals. The super-cell is chosen large enough to prevent interaction of neighboring cells. The structures are relaxed until the magnitude of maximum force on each atom becomes smaller than 0.02 eV/Å^3. Relaxation is followed by DFT calculations for evaluating the electronic structure. However, DFT is a ground state theory and is not appropriate for systems under excitations. According to the Runge-Gross theorem [12], the time dependent charge density $n(r,t)$ of a many-body system under external time dependent potential ($v_{\rm ext}(r,t)$) is a unique functional of the potential. This allows the treatment of response properties such as dynamic polarizability within DFT. Then the excitation energies and the oscillator strengths can be obtained as the poles and residues of the dynamic polarizability. By using a super-operator formulation of linearized time-dependent density-functional theory, the dynamic polarizability of an interacting-electron system is represented as an off-diagonal matrix element of the resolvent of the Liouvillian super-operator [13]. The oscillator strength indicates the number of electric dipole

978-1-4673-7860-4/15/$31.00 ©2015 IEEE

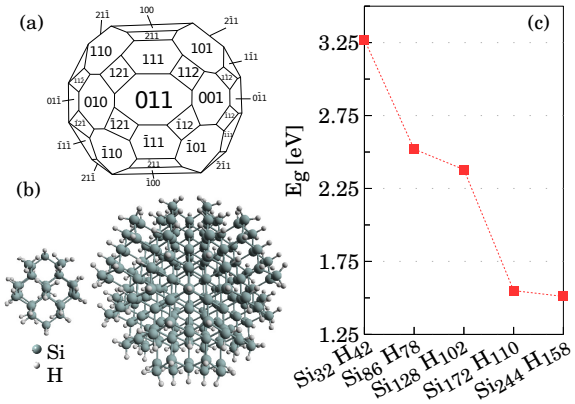

Fig. 1. (a) The model used for NC. (b) Hydrogen passivated Wulff-constructions: $Si_{32}H_{42}$ NC with a diameter of 1.2 nm and $Si_{244}H_{158}$ with a diameter of 2.2 nm. (c) HOMO-LUMO band-gaps based on DFT calculations for hydrogen passivated Si NCs with diameters in the range of 1.2-2.2 nm.

oscillators per molecule that are set in motion by the light field and oscillate with the characteristic frequency of the material.

The optical absorption spectra are obtained using the time dependent density functional perturbation theory (TDDFPT) calculations. This method is particularly well suited for large systems with large plane wave basis sets. TDDFPT calculations are carried out within the adiabatic approximation of exchange-correlation interactions, with linearization of the density matrix response using the Quantum ESPRESSO code [14]. The generalized gradient approximation with PBE exchange-correlation functionals, ultra-soft pseudo-potentials generated with Vanderbilt code, and the DZP plane wave basis set with a cutoff of 55 Ry have been used.

III. Results and Discussions

It is well known that quantum confinement (QC) and surface chemistry can modify the properties of NCs. If the size of NC becomes comparable to the Bohr radius, carrier energy gets quantized with a size-dependent trend similar to that of a particle in a box [3], [4]. In strong confinement regime ($r < a^*_{\mathrm{Bohr}}$), the band-gap of NC is inversely proportional to the diameter [4], [15]:

$$E_g^{QD}(d) = E_g^{\mathrm{bulk}} + \frac{A}{d^2}\ , \qquad (1)$$

where d is the diameter of NC in nanometer and A [eV.nm^2] is the fitting parameter [4]. We examined HOMO-LUMO band-gap variations for hydrogen passivated Si NCs with diameters in the range of 1.2-2.2 nm. Fig.1 clearly shows the inverse proportionality of the band-gap with the NC size. For the given diameter range and A=3.57 (strong confinement regime [4]), Eq. 1 predicts energy gaps in the range of 1.85-3.59 eV and our numerical analysis indicate bandgaps in the range of ∼1.5-3.25 eV which are in good agreement with previous works [5], [15], [16].

c) Spatial Position of Surface Passivant: Since NC facets have different surface energies they interact differently with the passivant atoms [17]. In addition, dissimilar facet boundaries and the broad range of inter-nuclear distances between the passivant and surface atoms of NC leads to

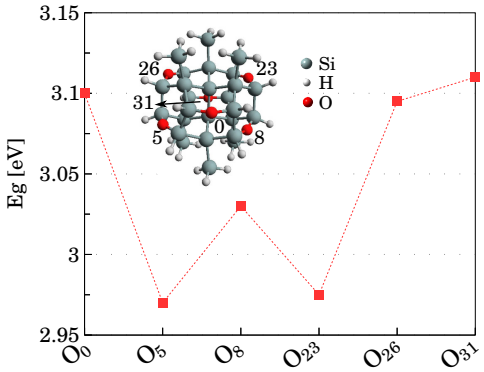

Fig. 2. The HOMO-LUMO band-gaps of $Si_{31}H_{40}O$ NCs with a single bridged oxygen surface passivant at various (100) facets.

various external potential profiles ($v_{\mathrm{ext}}(r,t)$) for the Kohn-Sham equation, which accordingly result in new eigenstates for the system. Thus, it is anticipated that the position of the surface passivants affects the optical and electrical properties of the NC. First we examine the effect of a single passivant atom placed at different positions of the surface of a $Si_{32}H_{42}$ NC with a diameter of 1.2 nm. A Si atom on a (100) facet is considered and its two bound hydrogen atoms are replaced with a bridged oxygen followed by the structure relaxation. The calculated HOMO-LUMO band-gaps are presented in Fig. 2 that show a variation of ∼0.15 eV for various positions of a single oxygen passivant.

The optical responses of the discussed structures are calculated using the TDDFPT method. For single bridged oxygen atom on a (100) facet, TDDFPT predicts an average optical gap of ∼6.5 eV with variations of the order of ∼0.55 eV for various passivation position (see Fig.3). The smaller HOMO-LUMO band-gap, in comparison with the optical gap is due to the well-known bandgap underestimation of DFT simulations [18].

d) Relative Position of Surface Passivants: To study the role of relative spatial position of surface passivants, four configurations are considered in which three bridged oxygen

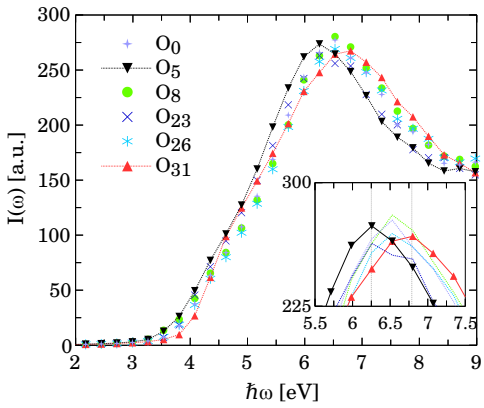

Fig. 3. Optical absorption spectra that are calculated using TDDFPT for $Si_{31}H_{40}O$ NCs with single bridged oxygen passivant atom at various (100) facets.

atoms with different relative positions are placed on the (100) facets of a $Si_{32}H_{42}$ NC, see the first column of Fig. 4. The relative position of terminants in $O_{0,5,23}$ configuration is symmetric, but with respect to the whole NC structure the surface termination is not symmetric (see subplots 1 and 4 in Fig. 4). The $O_{0,5,8}$ configuration is similar to the previous structure, but less symmetrical with respect to the relative position of the oxygen atoms (see subplots 16, 17 and 19 in Fig. 4). $O_{0,5,26}$ and $O_{0,5,31}$ configurations are similar with respect to the whole NC, while the relative position of passivants is mirrored.

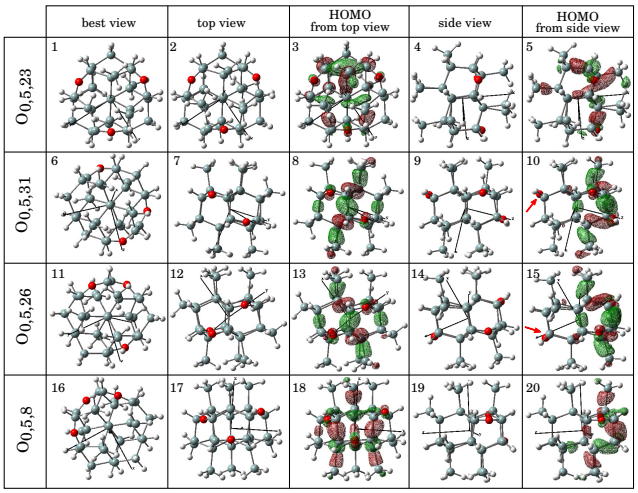

Fig. 4. The first column shows the cross-section of NC in the plane of the three oxygen atoms to represent their relative arrangement. Other columns show the density distribution of HOMO orbital and the corresponding cross-section of the NC. The column 'view 1', displays the plane on which the HOMO spreads. The column 'view 2' displays the view normal to the 'view 1', representing the plane on which the HOMO is localized. The density iso-surfaces are plotted at 0.033 electron/Å^3.

The oscillator strength spectra are calculated using TDDFPT simulations (see Fig.5). As expected, similar to the single-oxygen case, the optical transition energies are different for various surface passivation configurations. In this case the peak absorption energy varies ∼0.25 eV between the $O_{0,5,26}$ and $O_{0,5,31}$ configurations which show the maximum and minimum absorption peak energy, respectively. The referred structures are similar, except a mirrored relative position of oxygen atoms. As HOMO is the main electron donor, examining its density distribution can clarify the effect of relative position of passivants. For the sake of generality Fig. 6 compares HOMO/LUMO density maps for surface passivant species common in photovoltaics, including oxygen (bridged and double-bonded), NH_2, and CH_3 passivant groups. Fig. 6 indicates that the HOMO orbital is distributed all over the NC, while the LUMO orbital is localized at the center. Among the considered surface passivants the double-bonded oxygen resulted in the most localized orbital, followed by NH_2, bridged oxygen, and CH_3. Therefore, oxygen atom localizes the HOMO/LUMO orbitals of a Si NC more effectively than other common species in photovoltaics [7], [8], [19], [20]. Fig.7 shows the HOMO/LUMO energies and the oscillator strength spectra for passivation with single and multiple passivant groups. Fig.7(a) indicates that HOMO energies are raised with surface coverage and exhibit larger variations compared

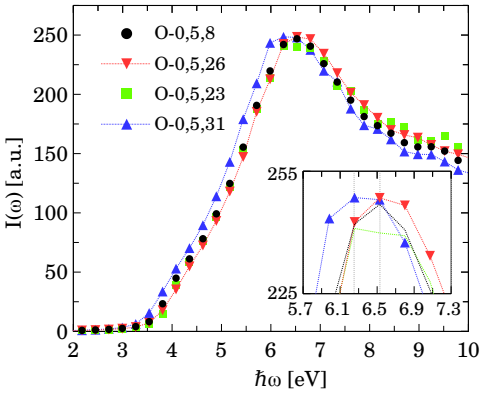

Fig. 5. TDDFPT predicted oscillator strength spectra for $Si_{29}H_{36}O_3$ NCs with various relative positions of three bridged oxygen passivants on (100) facets.

to LUMO. Surface coverage with oxygen and NH_2 reduces HOMO-LUMO band-gap [see Fig.7 (b)] which results in a red shift of the optical absorption spectra. A reduction in the absorption strength is also observed with surface coverage, however, the band-gap is not affected for the CH_3 group.

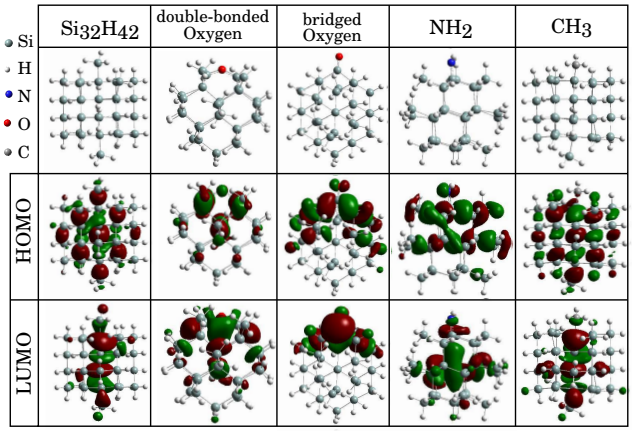

Fig. 6. The density iso-surfaces of HOMO orbital (iso-value of 0.033 [electron/Å^3]) for single bridged (double-bonded) oxygen atom, NH_2 and CH_3 groups on (100) facets of a $Si_{32}H_{42}$ NC.

Fig. 4 compares HOMO iso-surfaces of four different configurations. In the case of symmetric relative position of passivants (subplots 3 and 18) the HOMO spreads over all oxygen atoms, whereas in cases lacking such symmetries (subplots 10 and 15) the electronic cloud is localized on the two closer oxygen atoms and the third oxygen atom (shown with red arrow) is left out. It is known that oxygen atom can disturb the *sp* orbital network of a Si NC and results in the localization of the frontier molecular orbitals [7]–[9]. This is in agreement with our results that the HOMO electron cloud is mainly localized on oxygens. The comparison of subplots 3 and 18 (symmetric arrangement of oxygens) with subplots 8 and 13 (asymmetric arrangement of oxygens) reveals that the localization center of HOMO is mainly determined by the relative position of surface terminants. On the one hand, the

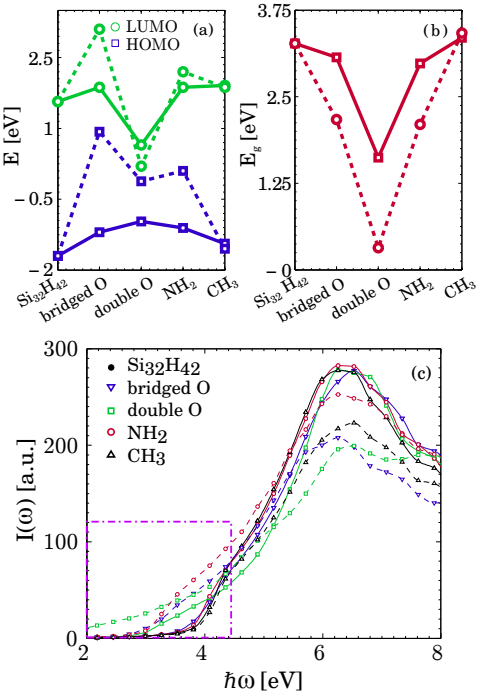

Fig. 7. (a) HOMO/LUMO energy variations, (b) band-gap variations, (c) oscillator strength spectra for single and multiple passivant groups of bridged and double-bonded oxygen, NH_2, and CH_3 on (100) facets of $Si_{32}H_{42}$ nanocluster. Solid lines correspond to single group passivation and the dashed lines represent the multiple group passivation.

localization center of orbitals determines the overlapping conditions and on the other hand optical transitions are determined by the overlap of frontier molecular orbitals.

IV. Conclusions

The effects of the spatial position and the relative position of bridged oxygen passtivants on the absorption spectra of hydrogen passivated Si NC are investigated. Examination of the HOMO-LUMO band-gap, oscillator strength spectra and the frontier molecular density distributions demonstrates that in addition to passivant material and surface coverage, the spatial position of each surface passivant and the relative position of passivants can significantly affect the localization center of frontier orbitals, which results in the variation of their overlap and the modification of optical transition energies. Previous studies have focused on chemical nature of surface passivation on NC properties. Our presented results, however, show that the role of spatial position and the geometrical arrangement of surface passivants cannot be neglected.

Acknowledgment

The computational results presented have been achieved in part using the Vienna Scientific Cluster (VSC).

References

[1] A. Feltrin and A. Freundlich, "Material considerations for terawatt level deployment of photovoltaics," *Renew Energy*, vol. 33, no. 2, pp. 180–185, 2008.

[2] H. Huff, *Into The Nano Era: Moore's Law Beyond Planar Silicon CMOS*, ser. Springer Series Mate. Springer Berlin Heidelberg, 2008.

[3] V. Kumar, K. Saxena, and A. Shukla, "Size-dependent photoluminescence in silicon nanostructures: quantum confinement effect," *Micro Nano Lett*, vol. 8, no. 6, pp. 311–314, 2013.

[4] E. G. Barbagiovanni, D. J. Lockwood, P. J. Simpson, and L. V. Goncharova, "Quantum confinement in si and ge nanostructures," *J App Phys*, vol. 111, no. 3, pp. 034 307–034 307–9, 2012.

[5] A. Nurbawono, S. Liu, and C. Zhang, "Modeling optical properties of silicon clusters by first principles: From a few atoms to large nanocrystals," *J chem phys*, vol. 142, no. 15, p. 154705, 2015.

[6] G. Seguini, C. Castro, S. Schamm-Chardon, G. BenAssayag, P. Pellegrino, and M. Perego, "Scaling size of the interplay between quantum confinement and surface related effects in nanostructured silicon," *Appl Phys Lett*, vol. 103, no. 2, pp. 023 103–023 103–5, 2013.

[7] A. Puzder, A. Williamson, J. Grossman, and G. Galli, "Surface chemistry of silicon nanoclusters," *Phys Rev Lett*, vol. 88, no. 9, pp. 097 401–097 401–4, 2002.

[8] A. Puzder, A. Williamson, J. C. Grossman, and G. Galli, "Passivation effects of silicon nanoclusters," *Mater Sci Eng: B*, vol. 96, no. 2, pp. 80–85, 2002.

[9] A. D. Zdetsis, S. Niaz, and E. N. Koukaras, "Theoretical study of oxygen contaminated silicon quantum dots: A case study for si 29 h 29- xo 29- y," *Microelectron Eng*, vol. 112, pp. 227–230, 2013.

[10] D. J. Lockwood and L. Tsybeskov, "Optical properties of silicon nanocrystal superlattices," *J Nanophotonics*, vol. 2, no. 1, pp. 022 501–022 501–33, 2008.

[11] J. M. Soler, E. Artacho, J. D. Gale, A. Garcia, J. Junquera, P. Ordejon, and D. Sanchez-Portal, "The siesta method for ab initio order-n materials simulation," *J Phys-Condens Matt*, vol. 14, no. 11, pp. 2745–2779, 2002.

[12] E. Runge and E. K. U. Gross, "Density-functional theory for time-dependent systems," *Phys Rev Lett*, vol. 52, pp. 997–1000, Mar 1984.

[13] D. Rocca, R. Gebauer, Y. Saad, and S. Baroni, "Turbo charging time-dependent density-functional theory with lanczos chains," *J Chem Phys*, vol. 128, no. 15, pp. 154 105–154 105–14, 2008.

[14] P. Giannozzi, S. Baroni, N. Bonini, M. Calandra, R. Car, C. Cavazzoni, D. Ceresoli, G. L. Chiarotti, M. Cococcioni, I. Dabo, A. Dal Corso, S. de Gironcoli, S. Fabris, G. Fratesi, R. Gebauer, U. Gerstmann, C. Gougoussis, A. Kokalj, M. Lazzeri, L. Martin-Samos, N. Marzari, F. Mauri, R. Mazzarello, S. Paolini, A. Pasquarello, L. Paulatto, C. Sbraccia, S. Scandolo, G. Sclauzero, A. P. Seitsonen, A. Smogunov, P. Umari, and R. M. Wentzcovitch, "Quantum espresso: a modular and open-source software project for quantum simulations of materials," *J Phys-Condens Mat*, vol. 21, no. 39, p. 395502 (19pp), 2009. [Online]. Available: http://www.quantum-espresso.org

[15] L. Brus, "Electronic wave functions in semiconductor clusters: experiment and theory," *J Phys Chem*, vol. 90, no. 12, pp. 2555–2560, 1986.

[16] K. Dohnalova, A. N. Poddubny, A. A. Prokofiev, W. D. de Boer, C. P. Umesh, J. M. Paulusse, H. Zuilhof, and T. Gregorkiewicz, "Surface brightens up si quantum dots: direct bandgap-like size-tunable emission," *Light Sci Appl*, vol. 2, no. 1, pp. e47–e47–6, 2013.

[17] H.-G. Liao, D. Zherebetskyy, H. Xin, C. Czarnik, P. Ercius, H. Elmlund, M. Pan, L.-W. Wang, and H. Zheng, "Facet development during platinum nanocube growth," *Science*, vol. 345, no. 6199, pp. 916–919, 2014.

[18] V. Kocevski, O. Eriksson, and J. Rusz, "Transition between direct and indirect band gap in silicon nanocrystals," *Phys Rev B*, vol. 87, no. 24, p. 245401, 2013.

[19] E. Ramos, B. M. Monroy, J. C. Alonso, L. E. Sansores, R. Salcedo, and A. Martinez, "Theoretical study of the electronic properties of silicon nanocrystals partially passivated with cl and f," *J Phys Chem C*, vol. 116, no. 6, pp. 3988–3994, 2012.

[20] S. M. Lee, K. J. Kim, D. W. Moon, and H. Kim, "Optical and electronic properties of hydrogenated silicon nanoclusters and nitrogen passivated silicon nanoclusters: A density functional theory study," *J Nanosci Nanotechno*, vol. 12, no. 7, pp. 5835–5838, 2012.